Journal of Controlled Release 377 (2025) 341–353

Contents lists available at ScienceDirect

Journal of Controlled Release

journal homepage: www.elsevier.com/locate/jconrel

Modulation of GABAergic neurons in acute epilepsy using sonogenetics

Thi-Nhan Phan [a,1], Ching-Hsiang Fan [b,c,1], Hsien-Chu Wang [d], Hao-Li Liu [e], Yu-Chun Lin [d,f,*], Chih-Kuang Yeh [a,**]

[a] Department of Biomedical Engineering and Environmental Sciences, National Tsing Hua University, Hsinchu 30013, Taiwan
[b] Department of Biomedical Engineering, National Cheng Kung University, Tainan 701401, Taiwan
[c] Medical Device Innovation Center, National Cheng Kung University, Tainan 701401, Taiwan
[d] Institute of Molecular Medicine, National Tsing Hua University, Hsinchu 30013, Taiwan
[e] Department of Electrical Engineering, National Taiwan University, Taipei 10617, Taiwan
[f] Department of Medical Science, National Tsing Hua University, Hsinchu 30013, Taiwan

ARTICLE INFO

Keywords:
Sonogenetics
GABAergic neuron
Epilepsy seizures
Ultrasound
Neuromodulation

ABSTRACT

Epilepsy, a neurological disorder caused by hypersynchronous neural disturbances, has traditionally been treated with surgery, pharmacotherapy, and neuromodulation techniques such as deep brain stimulation and vagus nerve stimulation. However, these methods are often limited by invasiveness, off-target effects, and poor resolution. We present a noninvasive alternative utilizing sonogenetics to selectively stimulate γ-aminobutyric acid (GABA)ergic neurons in the amygdala through engineered auditory-sensing protein, mPrestin (N7T, N308S), in a pentylenetetrazole-induced rat model. Activation of GABAergic neurons induced by the sonication with 0.5-MHz transcranial ultrasound can modulate epileptiform activity by 50 %. Electrophysiological recordings confirmed effective neuromodulation and persistent seizure suppression up to 60 min post-treatment without tissue damage, inflammation, or apoptosis. This sonogenetic approach offers a promising, safe method for epilepsy management by targeting GABAergic neurons.

1. Introduction

The development of noninvasive and high-precision neuromodulation techniques is crucial for treating neurological disorders such as epilepsy, which affects over 50 million globally with sudden-onset hypersynchronous neural disturbances [1]. Traditional epilepsy treatments include surgical resection, pharmacotherapy, and neuromodulation tools such as deep brain stimulation and vagus nerve stimulation. However, all these carry risks of invasive damage and off-target effects. Recent advances highlight the role of the intrinsic inhibitory neurotransmitter GABA (γ-aminobutyric acid) in deep brain amygdala GABAergic neurons as a key to mitigating epileptiform activities by inhibiting neuronal excitation [2]. To overcome the limitations of conventional epilepsy treatment, our approach utilizes GABAergic neurons targeted through transcranial focused ultrasound (US) and the engineered US-sensitive protein Venus-mPrestin (N7T, N308S) (Venus-mPrestin) [3–6] in sonogenetics for the precise and noninvasive suppression of epileptic activity.

Several methodologies have been developed for precisely manipulating targeted neuronal activity at the cellular level, including chemogenetics [7], optogenetics, and magnetogenetics leverage optics [8–11], chemicals [12–14], and magnetics [15]. However, each of these techniques has its own set of potential limitations: (1) optogenetics is constrained by a maximum tissue penetration depth of several centimeters; (2) chemogenetics could not offer the same level of control over timing and necessitates time to respond; and (3) while magnetogenetics offers noninvasive modulation of cellular activity, the requirement for additional magnetic nanoparticles and the poor spatial resolution of magnetic forces remain significant concerns. The localized and superior tissue-penetrating capability (several centimeters) of US-actuated

Abbreviations: GABA, γ-aminobutyric acid; US, ultrasound; PTZ, pentylenetetrazole; AP, anteroposterior; ML, mediolateral; DV, dorsoventral; ECoG, electrocorticography; AAV, adeno-associated virus; IHC, Immunohistochemistry; H&E, hematoxylin and eosin; TUNEL, terminal deoxynucleotidyl transferase biotin-dUTP nick end labeling.

* Corresponding author at: Institute of Molecular Medicine, National Tsing Hua University, Hsinchu 30013, Taiwan.
** Corresponding author.
E-mail addresses: ycl@life.nthu.edu.tw (Y.-C. Lin), ckyeh@mx.nthu.edu.tw (C.-K. Yeh).
[1] T.N. Phan and C.H. Fan contributed equally to this work.

https://doi.org/10.1016/j.jconrel.2024.11.029
Received 31 May 2024; Received in revised form 10 November 2024; Accepted 12 November 2024
Available online 23 November 2024

sonogenetics may offer a viable alternative to the current techniques.

Like optogenetics and magnetogenetics, sonogenetics relies on US-sensitive proteins to precisely activate targeted cell types or open exogenous US-sensitive ion channels on the cell membrane to modulate neuronal activity. Sonogenetic techniques have been refined to express US-sensitive ion channels such as TRP-4, MEC-4, Piezo1, TRPV1, TRAAK, TREK1, MEC-4 TRPA1, and MscL [6,16–25]. However, their deployment necessitates the use of microbubbles [16,22,23], high-frequency US [18,24,25], and multiple US stimulations [17,20,21,25]. These requirements may result in cavitation-induced damage or thermal

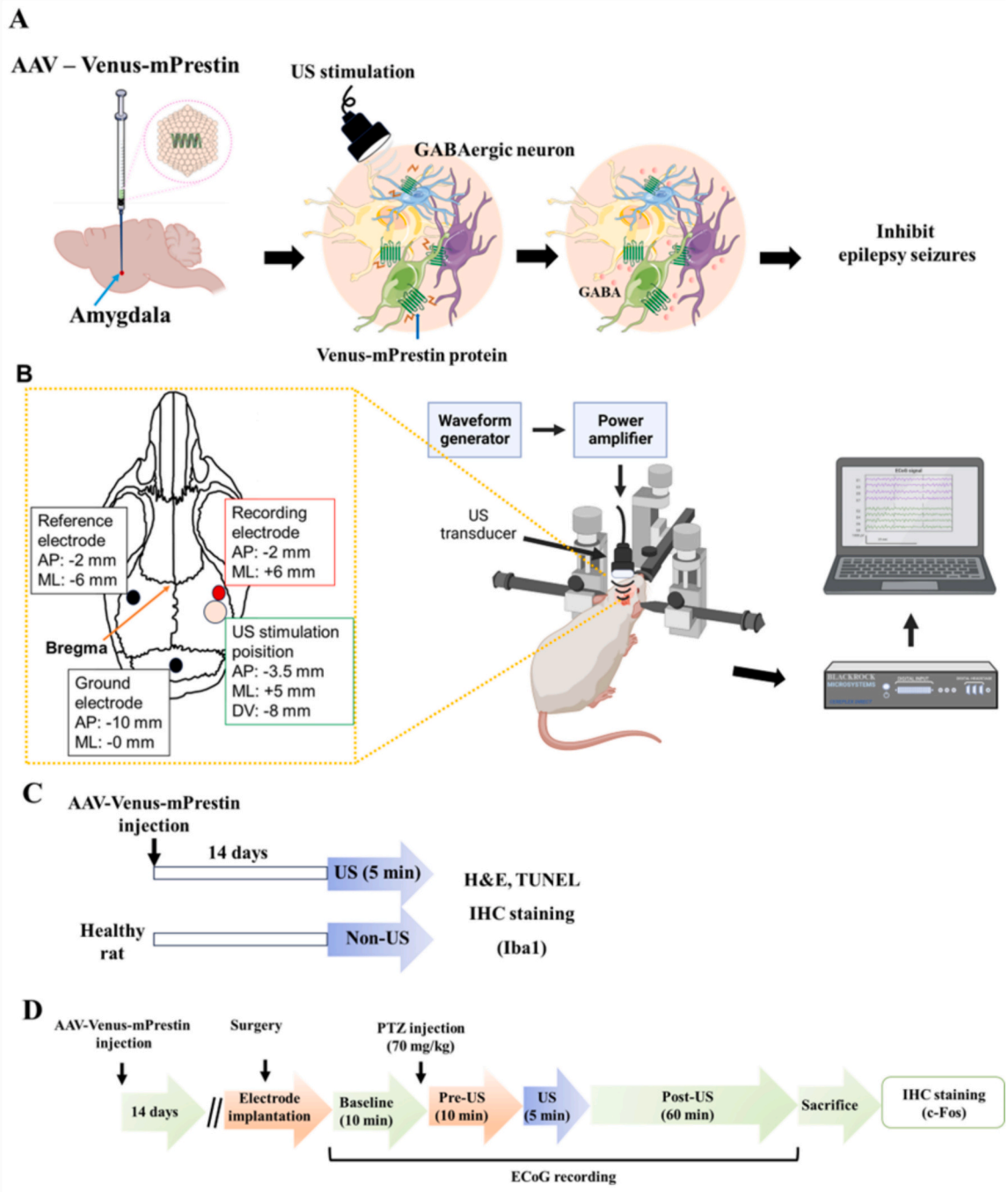

Fig. 1. Illustrations of the paradigm of this study. (A) The concept of this study. The US was used to selectively transcranial activate GABAergic neurons expressing Venus-mPrestin in the amygdala of epileptic animals, suppressing the overexcited neurons. The adeno-associated virus (AAV)-encoding Venus-mPrestin was injected into the right amygdala area (relative to bregma: anteroposterior [AP] = −3.5 mm, mediolateral [ML] = +5 mm, dorsoventral [DV] = −8 mm). (B) Illustration of the transcranial US stimulation system, the electrocorticography (ECoG) setup, and the implanted positions of the ECoG electrodes. The US was delivered to the right amygdala area (Figure created by BioRender.com). (C) The flowchart diagram of the safety verification experiment. The healthy rats were injected with AAV-Venus-mPrestin or treated with US stimulation before collecting the brain tissues to evaluate the brain damage by hematoxylin and eosin (H&E), terminal deoxynucleotidyl transferase dUTP nick end labeling (TUNEL), and Ionized calcium-binding adaptor molecule 1 (Iba1) staining. (D) The flowchart diagram of the epilepsy treatment experiment. Acute epilepsy seizures were induced by PTZ injection in Venus-mPrestin-expressing rats. Following 1-h electrode implantation, ECoG signals were recorded for 10 min as a baseline before injecting PTZ (baseline), an epilepsy state before US stimulation (10 min after PTZ injection, Pre-US), and through the 60-min post-US period).

effects in the US-targeted area that restrict their clinical application [26]. Our group recently proposed a sonogenetic approach to overcome the limitations inherent in existing sonogenetic methods. This strategy involves the genetic modification of prestin proteins (mPrestin) that are naturally expressed in the outer hair cells of the mouse cochlea and are essential for high-frequency hearing [3–6]. Ectopic expression of the engineered prestin enhances US sensitivity of targeted cells, enabling selective activation of dopaminergic neurons and alleviating symptoms of Parkinson's disease in mice [5].

While sonogenetics is a promising strategy for the minimally invasive, remote, and selective activation of targeted neurons in deep brain areas, its therapeutic efficiency in epilepsy remains to be verified. Here, we demonstrate this concept by using sonogenetics to selectively stimulate GABAergic neurons in the amygdala area and verify the effects of suppressing epileptic spikes in a pentylenetetrazole (PTZ)-induced acute epilepsy animal model (Fig. 1A). We then used c-Fos to verify if the mPrestin-expressing GABAergic neurons within the amygdala region could be stimulated by US or even modulate neuron activity in other brain regions *in vivo*. The impact of sonogenetics on epileptic spikes was evaluated by electrocorticography (ECoG) in real-time (Fig. 1B). The safety of this strategy was verified by histological examinations (Fig. 1C). The ECoG signals were recorded separately for the baseline state (10 min before PTZ injection), the epilepsy state or pretreatment period (10 min following PTZ injection), and the treatment state (60 min after US stimulation) (Fig. 1D).

2. Materials and methods

2.1. Animal husbandry

Experiments were conducted on 7 to 9-week-old Sprague Dawley (SD) male rats weighing 250–300 g (Lesco Biotech, Taipei, Taiwan). Rats were kept on a 12 h/12 h light/dark cycle (lights on at 07:00) and had access to food and water *ad libitum*. The institutional animal care and use committee at National Tsing Hua University approved the animal care and experimental procedures following NIH guidelines (IACUC approval number: NTHU110072).

2.2. Intracranial injections of AAV

Rats (7-week-old) were injected with adeno-associated virus (AAV)-Venus or AAV-Venus-mPrestin. The surgical area was sterilized using betadine and 75 % alcohol. Each rat was anesthetized with 3 % isoflurane (Panion & BF Biotech, Taipei, Taiwan) for 5 min before being placed in a stereotaxic instrument (David Kopf Instruments). Anesthesia was maintained by constantly administering 2 % isoflurane throughout the surgical procedure. A total of 3 μl of AAV-Venus-mPrestin or Venus-containing AAV (SSAAV9-CB-Venus core, Academica Sinica, New Taipei, Taiwan) (titer of 3.8×10^{13} vg/ml) was delivered transcranial into the right amygdala area (AP = −3.5 mm, ML = +5 mm, DV = −8 mm) of healthy rats *via* a Hamilton syringe. The needle was left in the injection position for 10 min to minimize the potential leakage of the injected solution. The incision was manually closed with sutures, and the rat was kept under a thermal lamp to maintain the body temperature during anesthesia and recovery. The AAV-Venus-mPrestin-injected rats (n = 21) were separated into four groups: (1) experiments evaluating AAV-Venus-mPrestin expression in the target brain area for different injected doses of AAV-Venus-mPrestin (n = 4), (2) the safety experiments (n = 6), (3) ECoG recording experiments (n = 10), and (4) rs-fMRI experiments evaluating AAV-Venus-mPrestin expression in the target brain area (n = 1).

2.3. Focused US setup and parameter design

AAV-Venus-mPrestin-infected cells in the epileptic animals were stimulated using a handmade single-element geometrically focused US transducer (center frequency = 0.5 MHz) comprising a piezoceramic disc (19.9 mm in diameter). The radius of curvature of this transducer is 20 mm (focal depth = 20 mm). The US pulses (pulse repetition frequency = 10 Hz, acoustic peak negative pressure = 0.5 MPa, 2000 cycles, mechanical index (MI) = 0.71, sonication duration = 5 min) were produced by a function generator (AFG3251, Tektronix, Beaverton, OR, USA) and fed to the US transducer *via* a radio-frequency power amplifier (Model 2100 L, Rochester, New York, USA). The US parameters used in this research were based on those identified in previous studies as optimal for activating Venus-mPrestin-expressing cells [4,5,27]. The US pressure amplitude and the acoustic field before and after delivering it through the skull, with and without placing the electrode on the rat skull in the target area, were measured by a calibrated hydrophone (HNC-0085 hydrophone, ONDA, Sunnyvale, USA) in a degassed water tank. The rat skull and electrode were positioned between the 0.5-MHz US transducer and the hydrophone (Fig. S1A—B). The acoustic energy of the 0.5-MHz US at the focal area through the rat skull with the electrode was 92 ± 1 % (Fig. S1C), which is comparable to the results (87 ± 7 %) reported by Kinoshita et al. [28]. The rat skull and the positioned electrode did not interfere with the beam pattern of the 0.5-MHz US beams (Fig. S1D—K).

2.4. Epileptic induction and ECoG setup

Acute epilepsy seizures were induced in 9-week-old SD male rats (n = 25) weighing 250–350 g (Lesco Biotech) by intraperitoneal injections of PTZ (70 mg/kg, Merck KGaA, Darmstadt, Germany). Animals were anesthetized with isoflurane at 3 % for inducing anesthesia and 1 % for maintaining anesthesia. All rats underwent surgery to expose their skull. After 14 days of AAV-Venus-mPrestin injection, the rats were anesthetized by isoflurane (3 %) and implanted bilaterally in three stainless-steel electrodes into the subdural space for acquiring ECoG signals over three positions: one background-position (AP = −10 mm, ML = 0 mm), one reference position (AP = −2 mm, ML = −6 mm), and one recording position (AP = −2 mm, ML = 6 mm) (Fig. 1B). After surgery to insert the electrodes, the rats rest for one hour under isoflurane anesthesia (1–2 %) before recording the ECoG signal. The ECoG signals were recorded for 10 min as a baseline before injecting PTZ, 10 min following the PTZ injection (epilepsy state or pretreatment period), and 60 min after US stimulation (post-US period) (Fig. 1D). Isoflurane was used to anesthetize rats during the experiments. After finishing the experiment, the rat was continuously anesthetized for 30 min to sacrifice for further histological analysis.

The ECoG signals were amplified, digitized at a sampling rate of 10,000 Hz by an AcqKnowledge 4.2 system (Biopac Systems, Goleta, CA, USA), and bandpass filtered at 1–80 Hz with a 60-Hz notch filter. MATLAB software (version R2021b, MathWorks, Natick, MA, USA) routines were used to analyze epilepsy spikes and bursts. A spike was defined as a sharp deflection with an amplitude at least 5 times higher than the background activity and a duration of at least 1000 ms. A burst was defined as more than three repetitive spikes within 1 s. The burst duration was calculated from the start of the first spike to the end of the last one.

To evaluate the effects of US and Venus-mPrestin on the PTZ-induced epilepsy rat model with ECoG signals, rats were separated into five groups: (1) Healthy animals used for comparisons (healthy group, n = 5), (2) PTZ-injected animals without receiving treatment (untreated group, n = 5), (3) PTZ-injected animals receiving US stimulation only (US group, n = 5), (4) PTZ-injected animals receiving Venus-mPrestin administration (Venus-mPrestin group, n = 5), and (5) PTZ-injected animals receiving both with Venus-mPrestin and US (Venus-mPrestin+US group, n = 5). A custom-made holder placed the US transducer on the top of the rat skull to deliver US to the targeted area in the rat brain. The rats were anesthetized and fixed on a stereotaxic instrument during US stimulation.

2.5. Histology experiments

The effects of US stimulation and/or AAV-Venus-mPrestin injection on brain tissue were evaluated using histological assays. The hematoxylin and eosin (H&E), terminal deoxynucleotidyl transferase dUTP nick end labeling (TUNEL), and ionized calcium-binding adaptor molecule 1 (Iba1) stains were performed after 5 min following US stimulation or 14 days after AAV-Venus-mPrestin injection (Fig. 1C). The US-stimulated rats and AAV-Venus-mPrestin-expressing rats were anesthetized with isoflurane and sacrificed *via* transcranial perfusion with normal saline and a 1 % formalin solution. The brain was extracted and immersion-fixated in 10–30 % sucrose for 24 h each before being frozen in a water-soluble blend of glycols and resins solution at −20 °C. Tissue sections were cut on a cryostat to prepare the histological slices for producing 20-μm-thick slices of brain tissue. Hemorrhage extravasation and apoptotic cells were detected using staining with H&E (Abcam, Waltham, MA, USA) and TUNEL Assay Kit (BrdU-Red, ab66110, Abcam), respectively. A fluorescence microscope (Ti2, Nikon, Tokyo, Japan) was then used to image the stained sections with the aid of 4× and 60× objectives (Nikon). The activated microglia and macrophages were detected by Iba1 polyclonal antibody (1:100, PA5–21274, ThermoFisher Scientific) at 4 °C overnight. After rinsing in PBS, the sections were incubated for 1 h at room temperature with goat anti-rabbit IgG H&L (Alexa Fluor® 594) secondary antibody (1:100, ab150080, Abcam) and then labeled with 4′,6-diamidino-2-phenylindole (DAPI) dye (Calbiochem, San Diego, CA, USA) dye to identify the nuclei. The number of $Iba1^+$ cells and the proportion of $Iba1^+$/$DAPI^+$ cells were determined in sections selected, and images were quantified to evaluate the $Iba1^+$ cells.

2.6. Immunohistochemistry experiments

Immunohistochemistry (IHC) co-labeling was performed to verify whether the AAV-Venus-mPrestin was successfully transfected into GABAergic neurons. Following 14 days of AAV-Venus-mPrestin injections, the rat brains were collected and kept in 4 % paraformaldehyde. After slicing the brain into 20-μm-thick slices, the sections were stained overnight at 4 °C within the mixture of two primary antibodies (Chicken-anti GFP antibody [1:100, GTX13970, Gentex] and Mouse monoclonal [K-87] to GAD_{67}/GAD_1 [1:100, ab26116, Abcam]). The sections were rinsed in PBS and then incubated for 1 h at room temperature with the mix of two-second antibodies (Goat Anti-Chicken IgY H&L (Alexa Fluor® 488) [1:200, ab150169, Abcam] and Goat Anti-Mouse IgG H&L (Alexa Fluor® 647) [1:200, ab150115, Abcam]). The sections were washed with PBS before being labeled with DAPI dye to identify the nuclei.

The intracerebral expression of AAV-Venus-mPrestin and the transfection efficiency of Venus-mPrestin to GABAergic neurons in the left amygdala area were evaluated by the percentages of $Venus^+$/GAD_{67}^+ cells and $Venus^+$ cells. Four coronal slices were collected from each animal. The slices were separated by 250 μm, and three or four regions of interest (ROIs, measuring 250 μm by 250 μm) were imaged in each. We counted the number of Venus-mPrestin-expressing (green fluorescence) and GAD_{67}-expressing (red fluorescence) cells to estimate the percentages of $Venus^+$/GAD_{67}^+ cells and $Venus^+$ cells. The $Venus^+$/GAD_{67}^+ cells could be distinguished using an overlapping mask between two channels (green or red fluorescence channel). ImageJ software was used to accurately quantify double-positive cells. The effective activation of neuron cells after treatments was confirmed using the c-Fos antibody (1:100, PA5–143600, ThermoFisher Scientific). The number of $c\text{-}Fos^+$ cells and the proportion of $c\text{-}Fos^+$/$DAPI^+$ cells were determined in the sections selected, and images were quantified to evaluate the $Venus^+$/$GABA^+$ cells.

2.7. Analysis methods

The ECoG data were analyzed using MATLAB software. Statistical analyses were performed using Prism software (GraphPad Software, San Diego, CA, USA). ECoG data were analyzed statistically using the two-way analysis of variance (ANOVA) and Tukey correction with a *p*-value significance criterion of <0.05. Indices were compared in the various experimental groups according to the normalized seizure results. Data are mean ± SEM (standard error of the mean) values. Two-way ANOVA was used to compare the spike number, burst number, burst duration, and the spike numbers of each extracted ECoG brainwave (alpha, theta, beta, delta, and gamma) between PTZ-induced rats untreated with PTZ-induced rats treated with US only, Venus-mPrestin-only, or Venus-mPrestin+US. Tukey's post-hoc tests were applied to understand group differences following ANOVA completely. At each time point, the spike number, burst number, burst duration, and the spike numbers of each extracted ECoG brainwave (alpha, theta, beta, delta, and gamma) at different experiment groups were compared using one-way ANOVA with Tukey's multiple comparison test. One-way ANOVA with Tukey's multiple comparison tests was also used to compare the spike number, burst number, burst duration, and the spike numbers of each extracted ECoG brainwave (alpha, theta, beta, delta, and gamma) at different time points post-treatment relative to the pre-treatment period in each experimental group. A *p*-value of less than 0.05 is regarded as significant. Two-way ANOVA and Tukey correction with a significance criterion of $p < 0.05$ were employed for histology analyses.

3. Results

3.1. In vivo expression of Venus-mPrestin in GABAergic neurons

We first evaluated the expression of Venus-mPrestin within the amygdala area by microscopy imaging after performing 14 days of intracerebral injections of AAV-encoding Venus-mPrestin into the amygdala area using different injection volumes (1, 3, and 5 μl). The mPrestin was fused with the gene encoded by the Venus yellow fluorescent protein to enable the visualization of its intracerebral distribution. Scattered Venus-mPrestin signals were observed in the expected location for the 1-μl injection (Fig. 2A-B). The distribution of Venus-mPrestin signals increased with the injection volume, being 402, 908, and 1587 a.u. for 1, 3, and 5 μl, respectively, with no Venus signal detected in a none-sonicated brain (294, 357, and 365 a.u. for 1, 3, and 5 μl, respectively (Fig. 2A-B). A large Venus-mPrestin signal appeared outside the amygdala area for the 5-μl injection, suggesting that such a high dose would induce severe off-target effects of the gene delivery. We also assessed whether the injected AAV-Venus-mPrestin would elicit an immune response by identifying the appearance of microglia (labeled by Iba1 antibody in red fluorescence) with IHC imaging. The microscopic images showed that injecting 1–3 μl only slightly activated microglia infiltration at the injection site compared with healthy rats (Fig. 2A). However, there was a significant increase in the number of microglia in the injected parenchyma when the injection dose was increased to 5 μl. Quantitative analysis of the microscopic images confirmed that the immune response was a significant difference between different injection volumes ($F\ [DFn, DFd] = F\ [4, 175] = 27.51$; $p < 0.0001$). Tukey post-hoc tests revealed that the 5 μl dose (3.7 ± 0.3 %; mean ± SEM) was larger than the dose of 1 μl (1.7 ± 0.2 % [$p < 0.0001$]) and the dose of 3 μl (1.5 ± 0.5 % [$p < 0.0001$]) (Fig. 2C). Therefore, we selected a 3-μl injection dose for the subsequent experiments. Besides, the diameter and length of the 0.5-MHz US focal point were 4 and 22 mm, respectively (Fig. S1D—K), sufficient to cover the Venus-mPrestin-expressing brain area.

After optimizing the injection volume for Venus-mPrestin expression, we evaluated whether the Venus-mPrestin specifically expresses in GABAergic neurons (labeled by GAD_{67} antibody in far-red fluorescence). The microscopic IHC images of the amygdala revealed that 89.3 ± 1.8 % of GAD_{67}-positive GABAergic neurons exhibited Venus-mPrestin signals ($Venus^+$/GAD_{67}^+ cells or $Venus^+$ cells), as evidenced by strong colocalization between Venus-mPrestin signals and GAD_{67} signals (pink

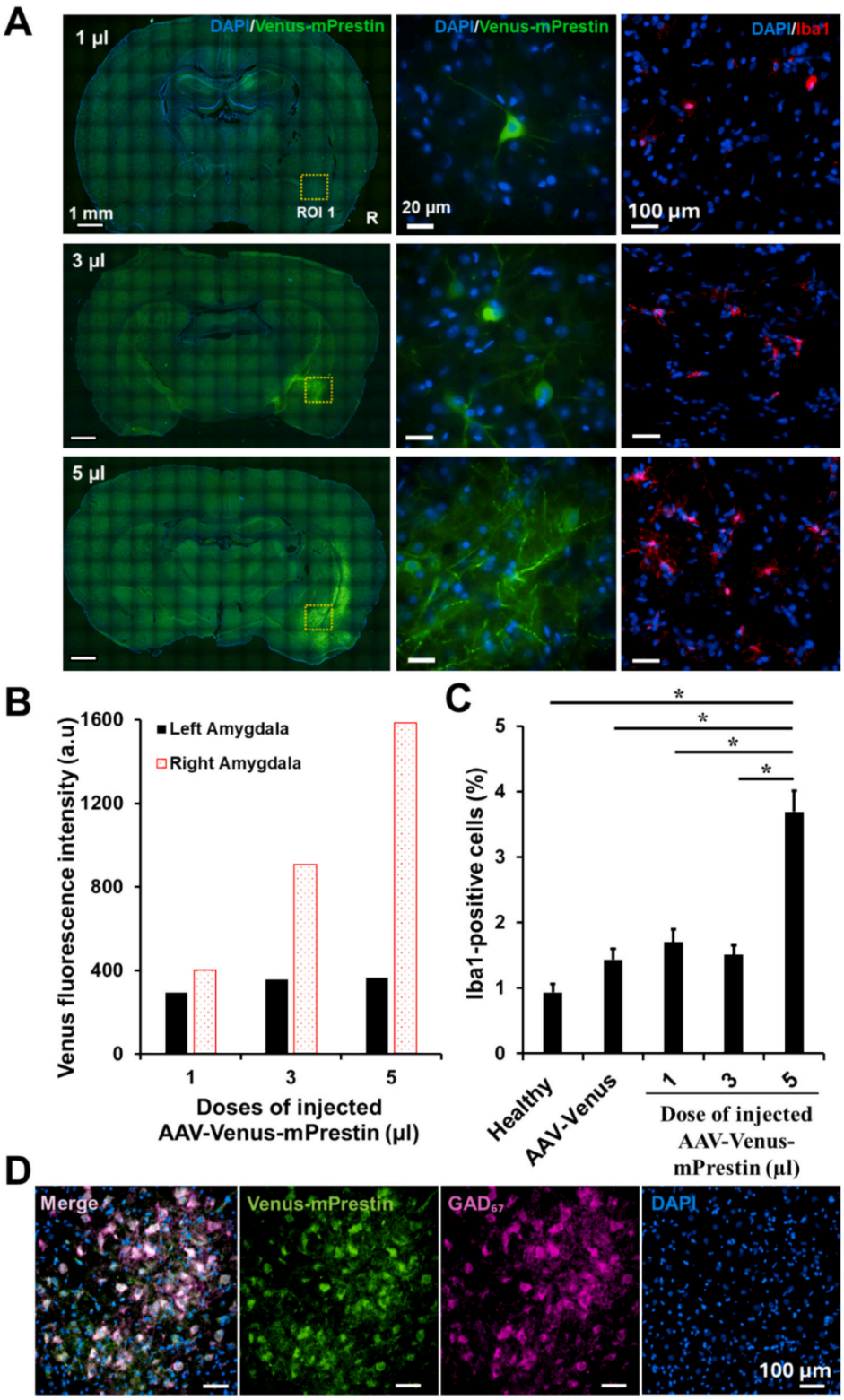

Fig. 2. (A) Left: whole-brain sections showing the intracerebral expression of Venus-mPrestin after 14 days for different AAV injection doses (1, 3, and 5 µl) in the amygdala area. Middle panel: magnified views of the indicated ROIs. Right panel: IHC images of microglia activation (labeled by Iba1 antibody in red fluorescence) in the indicated ROIs. (B) Quantification of Venus-mPrestin intensity in AAV-injected right Amygdala (red) and collateral sites (black) ($n = 1$ per group). (C) Quantification of red fluorescence intensity (microglia activation) in brain tissues under the indicated conditions ($n = 3$ per group). Data are presented as mean ± SEM from three independent experiments. (One-way ANOVA analysis with Tukey correction; *, $p < 0.05$). (D) The brain sections were used to detect the expression of Venus-mPrestin in GABAergic neurons, which were labeled by the GAD_{67} antibody in far-red fluorescence (n = 3 per group). (For interpretation of the references to color in this figure legend, the reader is referred to the web version of this article.)

fluorescence) (Fig. 2D). This result suggests that Venus-mPrestin was successfully and specifically expressed in GABAergic neurons. Besides, we found that most Venus-mPrestin-expressing cells are normal neurons (100 %, NeuN-positive neurons). The Venus-mPrestin expression was detected mainly in GABAergic neurons (75.5 ± 2.4 %), especially parvalbumin neurons (51.8 ± 12.2 %), but rarely in VGLUT1-positive glutamatergic neurons (4.7 ± 3.9 %) (Fig. S2).

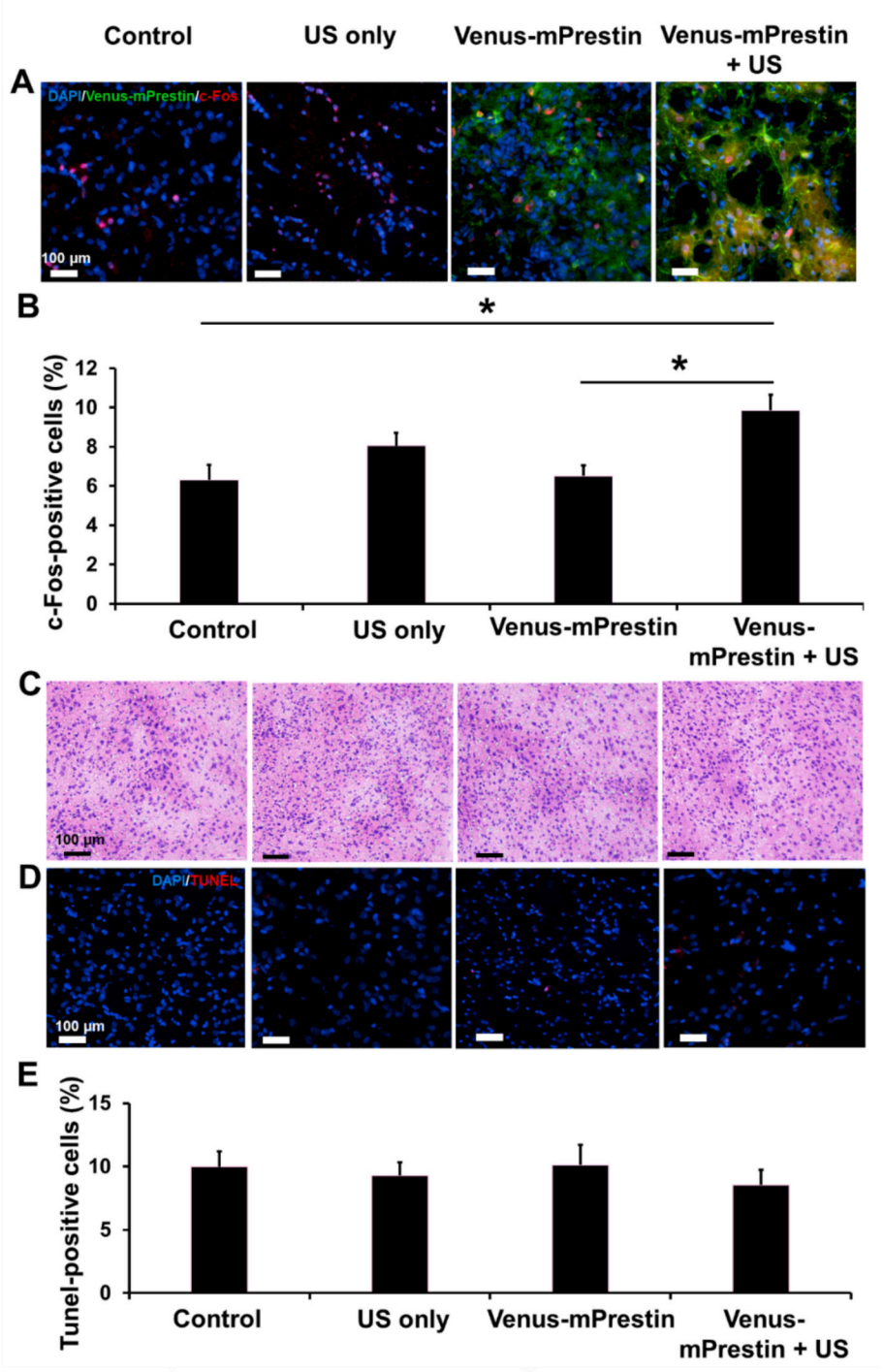

Fig. 3. (A) The c-Fos expression (red color) was used to evaluate neuron activity in the control or Venus-mPrestin-expressed amygdala area with or without US stimulation. Orange color: overlap of the Venus-mPrestin signal (green color) and the c-Fos signal (red color). Cell nuclei were labeled by DAPI staining (blue color). (B) Numbers of c-Fos$^+$ cells in each group ($n = 3$ rats per group from 2 independent experiments). Data are shown as mean ± SEM. Statistics: One-way ANOVA, Tukey correction. *, $p < 0.05$. (C) H&E staining was used to visualize the occurrence of erythrocyte extravasation in the amygdala area receiving the indicated treatments. (D) TUNEL staining was used to detect the occurrence of cell apoptosis in the amygdala area. (E) Numbers of TUNEL-positive cells (n = 3 per group). Statistics: One-way ANOVA, Tukey correction. *, $p < 0.05$. The difference between the experiment group and the control group was found. (For interpretation of the references to color in this figure legend, the reader is referred to the web version of this article.)

3.2. Sonogenetics can selectively activate Venus-mPrestin-expressing brain area

We next verified whether the Venus-mPrestin-expressing GABAergic neurons within the amygdala region could be stimulated by US or even modulate neuron activity in other brain regions *in vivo*. The c-Fos staining data shows that the c-Fos-positive cells in the Venus-mPrestin+US group (9.8 ± 0.8 %) were higher than other groups (F [3, 140] = 5.39; $p = 0.0015$), including the US-only group (8.0 ± 0.7 %, $p = 0.28$), Venus-mPrestin only group (6.5 ± 0.6 %, $p = 0.006$), and control group (6.3 ± 0.8 %, $p = 0.003$) (Fig. 3A-B). It indicated that US can selectively activate Venus-mPrestin-expressing GABAergic neurons. The c-Fos-positive cells in the US-only group (8.0 ± 0.7 %) are higher than the control group, even though there is no significant difference ($p = 0.31$). This result is demonstrated by several studies that indicate the capacity of US to activate neuron activities [29,30]. Besides, we also performed the c-Fos staining from the Venus-mPrestin+US rats at different brain regions (amygdala, hippocampus, putamen, and thalamus areas in two hemispheres). The results showed significant differences between hemispheres for a series of brain slides (F [3,210] = 45.29; $p < 0.0001$). The number of c-Fos positive cells in the US-stimulated area (the right amygdala region) is significantly higher (13.4 ± 0.8 %, $p < 0.0001$) compared to other brain regions both in the US passing regions and the contralateral brain regions (right hippocampus: 0.2 ± 0.1 %, $p < 0.0001$; right putamen: 2.8 ± 1.1 %, $p < 0.0001$; right thalamus: 0.9 ± 0.3 %, $p < 0.0001$; left amygdala: 2.0 ± 0.7 %, $p < 0.0001$; left hippocampus: 0.2 ± 0.1 %, $p < 0.0001$; left putamen: 0.1 ± 0.1 %, $p < 0.0001$; left thalamus: 1.0 ± 0.3 %, $p < 0.0001$;) (Fig. S3). These results confirmed that US can selectively activate Venus-mPrestin-expressing GABAergic neurons.

We further performed resting-state functional magnetic resonance imaging (rs-fMRI) to observe *in vivo* brain regional activity changes before, during, and after US stimulation. Note that the rs-fMRI experiment had a sample size of 1, only serving as preliminary data to support our hypothesis. In the Venus-mPrestin+US group, higher signals appeared in the US-stimulated amygdala than in other brain areas (Fig. S4A), similar to the c-Fos observations (Fig. 3A-B). Besides, in the functional connectivity matrix, the connectivity is strongly enhanced in the Venus-mPrestin+US group in the caudate putamen (CPu)/amygdala region (Fig. S4B) compared to other groups. It also supports the Venus-mPrestin effectively enhanced the US brain-stimulating effect. US stimulation also propagated the effects of Venus-mPrestin to the left hemisphere and influenced connectivity within brain regions, particularly with the thalamus and cortical regions (Fig. S4B). This effect may be mediated through the inhibitory control mechanisms in these previously identified pathways, ultimately contributing to the suppression of epileptic activity. It also indicated that the expression of Venus-mPrestin might not induce spontaneous neuron activation. We also found an enhancement in neuron activity in the right hemisphere of the US-only group, even though there was no significant difference, which is consistent with previous reports of US-modulating neuron activity under different conditions [31]. Quantification of the BOLD signals showed that they were maximal for the Venus-mPrestin+US condition, suggesting our proposed technique could stimulate *in vivo* brain-expressed Venus-mPrestin area.

In addition, several studies have shown that US overexposure can damage brain tissues and induce DNA breaks [32]. To assess any tissue damage induced by our sonogenetic stimulation, the stimulated brain tissues underwent H&E and TUNEL staining to evaluate erythrocyte extravasation and cell apoptosis, respectively. No noticeable structural disruptions in tissues and erythrocyte extravasation were observed in any group for the coronal sections of the amygdala area H&E staining after stimulation (Fig. 3C). In TUNEL staining, there were no significant intergroup differences in the number of TUNEL-positive cells between groups (F [3, 140] = 0.32; $p = 0.81$), which in the healthy, US-only, Venus-mPrestin only, and Venus-mPrestin+US groups are 9.9 ± 1.2 % ($p = 0.86$), 9.3 ± 1.0 % ($p = 0.97$), 10.1 ± 1.6 % ($p = 0.82$), and 8.5 ± 1.2 %, respectively (Fig. 3D-E). These suggest that stimulation at the employed parameters did not damage brain neurons.

3.3. Sonogenetics can suppress epileptic spikes in epilepsy animals

After confirming that Venus-mPrestin+US could activate the GABAergic neurons and affect the activity in other brain regions, we investigated the feasibility of applying this strategy to suppress epileptic spikes *in vivo*. Epilepsy was induced in rats by injecting PTZ intraperitoneally (IP) since PTZ has been widely used to induce acute epileptic-like neuron discharges in the whole brain [33–35] (Fig. 4A). Fig. 4B presents representative ECoG data collected from brains receiving different treatments, showing raw ECoG signals and the identified spikes. No unusual ECoG signals appeared when PTZ was not injected, whereas several epileptic spikes were detected following PTZ injection, indicating the successful induction of epilepsy in the animals. Treating epileptic animals with either US only or Venus-mPrestin injection only did not result in any obvious variations in the induced epileptic spikes. However, in epileptic animals expressing Venus-mPrestin, the number and amplitude of epileptic spikes obviously decreased after US stimulation. This shows that the occurrence of epileptic spikes induced by PTZ injection can be suppressed by our proposed sonogenetic strategy. Furthermore, these data also confirmed the high stability of Venus-mPrestin expression in the brain since it did not interfere with the brainwaves without US stimulation.

Fig. 5 provides a detailed comparison of the spike counts, burst counts, and burst durations between before and after performing different treatments for 60 min. Before the treatments, all PTZ-injected animals exhibited increased ECoG spikes compared with the healthy group: 0.7 ± 0.1, 4.5 ± 1.4, 3.9 ± 1.5, 3.0 ± 0.9, and 3.1 ± 0.8 spikes in the healthy, untreated, US-only, Venus-mPrestin only, and Venus-mPrestin+US groups, respectively (Fig. 5A). No significant difference was observed between the untreated and US-only groups at any time points (F [6,48] = 0.16, $p = 0.99$). There was a slight decrease in the number of spikes in the Venus-mPrestin-only group, from 3.0 ± 0.9 spikes pretreatment to 2.2 ± 0.6 spikes at 60 min posttreatment, $p = 0.03$ (F [6,24] = 2.9). Venus-mPrestin+US induced the largest spike-suppressive effect, with a 53.81 % spike reduction compared with the untreated group from 20 to 60 min post-US (F [6,48] = 3.4, $p = 0.008$). The epileptic suppression effect of 53.8–57.9 % reductions in the epileptic spikes was maintained for 60 min after US stimulation. We also found that the number of spikes reduced significantly by 46.5–52.4 % between before and after the treatment in the Venus-mPrestin+US group (F [6,24] = 6.92, $p = 0.0002$).

Similar to the spike count, the burst count in all PTZ-injected animals was largely increased compared with the healthy group: 0.7 ± 0.2, 1.4 ± 0.4, 1.3 ± 0.4, 1.5 ± 0.3, and 0.9 ± 0.3 bursts in the healthy, untreated, US-only, Venus-mPrestin only, and Venus-mPrestin+US groups, respectively (Fig. 5B). The burst counts did not change during the experimental timeline in any group (F [34, 140] = 1.5, $p = 0.06$). However, there was a slight decrease in the burst count in the Venus-mPrestin+US, with a 46 % burst reduction compared with the untreated group at 60 min post-US (F [6,48] = 3.4, $p = 0.008$). The Venus-mPrestin+US group showed a significant decrease in burst duration, from 9.9 ± 3.9 s pretreatment to 2.3 ± 0.4 s at 50 min after the US stimulation (F [6,24] = 2.6, $p = 0.05$) (Fig. 5C). There was no significant difference in burst duration in the healthy, untreated, US-only, and Venus-mPrestin-only groups between before and after treatment: from 1.1 ± 0.1 to 1.9 ± 0.2 s (F [6,24] = 0.19, $p = 0.97$), from 9.2 ± 2.2 to 5.3 ± 2.7 s (F [6,24] = 0.27, $p = 0.95$), from 5.7 ± 3.6 to 2.9 ± 0.6 s (F [6,24] = 0.46, $p = 0.83$), and from 4.1 ± 0.9 to 2.0 ± 0.4 s (F [6,24] = 1.9, $p = 0.12$), respectively (Fig. 5C).

Since previous studies have found that ictal epilepsy would also induce changes of brainwaves in different frequency bands, such as delta (0.5–4 Hz), theta (4–8 Hz), alpha (8–13 Hz), beta (13–30 Hz), and

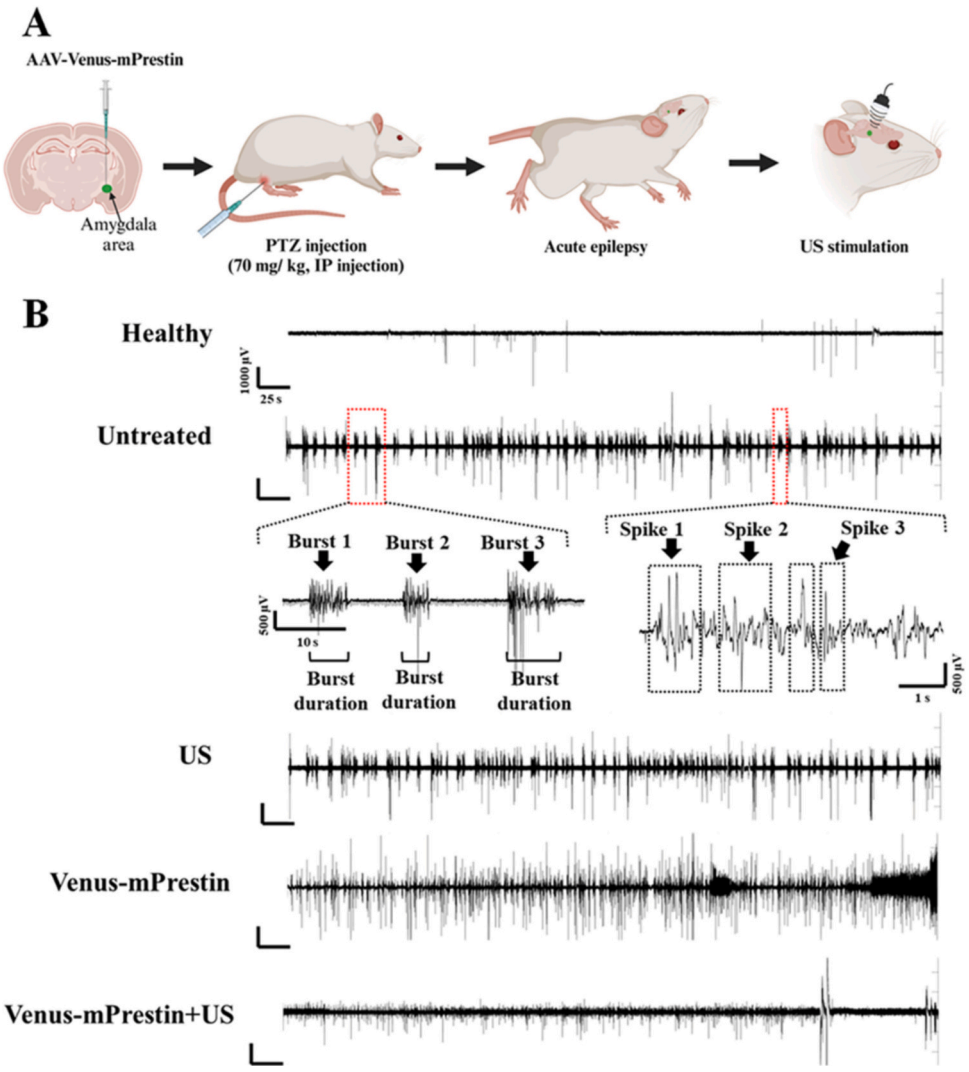

Fig. 4. (A) Using transcranial US stimulation of the Venus-mPrestin-expressing amygdala area to reduce epileptic spikes in PTZ-administered rats (Figure created by BioRender.com). (B) Representative ECoG recordings in brains under different conditions: healthy, untreated rats, US-only, Venus-mPrestin only, and Venus-mPrestin+US groups.

gamma frequency (40–100 Hz) [36,37], we further analyzed the brainwave variance in different frequency bands after treatment. Before the treatment, the peak spike counts in the delta, theta, and alpha bands increased significantly in all groups, accompanied by increased power within these bands. This brainwave elevation persisted throughout the experimental timeline in the untreated, US-only, and Venus-mPrestin-only groups. However, after treatment with Venus-mPrestin+US, there was a significant reduction in spike counts in the alpha band in both from the pretreatment levels ($F\ [6,24] = 6.92$, $p = 0.0002$) decreasing from 3.1 ± 1.6 to 1.7 ± 0.4 spikes at the posttreatment and compared to the untreated group ($F\ [6,48] = 2.72$, $p = 0.02$), from 3.7 ± 0.6 to 1.6 ± 0.4 spikes. In the delta band, the Venus-mPrestin+US group exhibited a significant decrease in spike counts before and after treatment ($F\ [6,24] = 6.72$, $p = 0.0003$) (Fig. 6A-C). Additionally, there was no significant difference between pretreatment and posttreatment levels in the theta, beta, and gamma brainwaves across all experimental groups (theta: $F\ [24, 120] = 0.85$, $p = 0.53$; beta: $F\ [24, 120] = 0.34$, $p = 0.95$; and gamma: $F\ [24, 120] = 0.9$, $p = 0.6$), including the Venus-mPrestin+US group (Fig. 6B-E).

The neuronal activities in the stimulated amygdala area of the epileptic rats after the sonogenetic treatment were verified by c-Fos staining. The number of the c-Fos-positive cells between groups shows a significant difference ($F\ [4, 235] = 8.9$; $p < 0.0001$). The untreated epileptic rats showed significant increases in c-Fos$^+$ neurons (26.9 ± 1.4 %) compared to the healthy rats (16.1 ± 1.3 %) ($p < 0.0001$) (Fig. 7). At the same time, this slightly decreased in epileptic rats in the US-only and Venus-mPrestin-only groups (21.3 ± 1.5 % [$p = 0.035$] and 22.4 ± 1.6 % [$p = 0.15$], respectively). Venus-mPrestin-expressing animals receiving US treatment showed a significant decrease in c-Fos$^+$ neurons (18.2 ± 1.2 %) ($p = 0.0001$) in the amygdala compared with the untreated rats but no significant difference relative to healthy rats ($p = 0.83$). These results were consistent with the above-mentioned electrophysiological recordings, confirming that sonogenetics can reduce the activity of the hyperexcitable neurons in epileptic animals.

4. Discussion

US has been recently proposed as a promising approach for non-invasively treating neurological disorders, especially epilepsy [38]. There are two major mechanisms for explaining US-induced epileptic spike suppression in clinical applications. First, high-intensity US can directly destroy or ablate hyperexcitable neurons in the hypothalamus to inhibit epilepsy seizures [38,39]. However, this method requires accurately delivering large amounts of energy to extremely localized areas. The intrinsic geometry of the skull can significantly distort where applied US is focused, potentially resulting in damage to nontarget

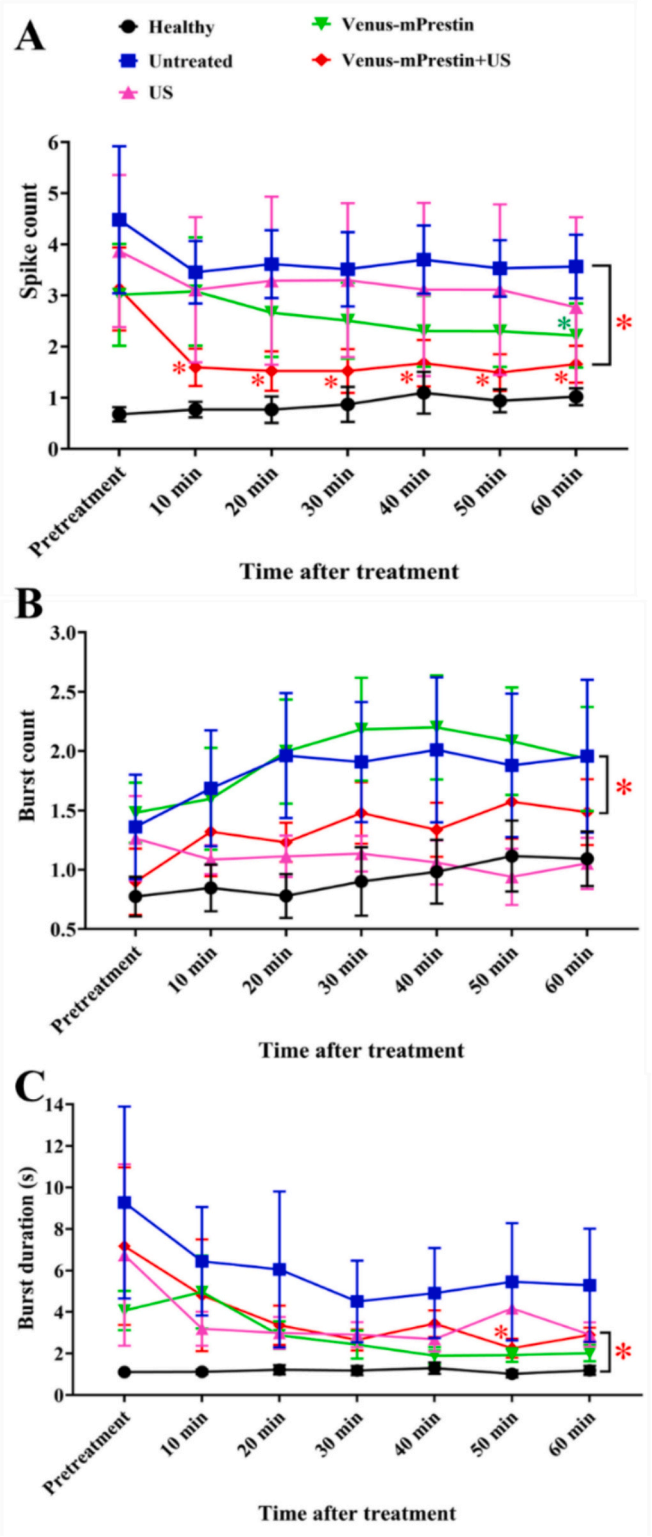

Fig. 5. Quantification of epileptic ECoG signal spikes under different treatment conditions: (A) spike count, (B) burst count, and (C) burst duration. Data are mean ± SEM values of five animal groups. Statistics: Two-way ANOVA, Tukey correction. *, $p < 0.05$. The asterisk color indicated the group marked with the corresponding color.

tissues. Second, low-intensity US can modulate neuronal activity by interfering with the cellular membrane's ion channels or synaptic transmission. However, the submillimeter spatial resolution of US stimulation may activate different types of neurons or multiple brain circuits simultaneously, potentially reducing the treatment effect. Therefore, most studies have used large amounts of energy (30–50 % of duty cycle [30,40–42], long treatment times (10–30 min [29,42–44], and multiple stimulations (two to four times [30,39,45,46]) to achieve treatment effects. However, the suppression effects of US stimulation on epilepsy were short-lived (20–30 min) [42,45,46], or their durations were not reported [41]. To overcome the trade-offs faced by using traditional US for epilepsy treatment, we propose sonogenetics as an alternative option because this method can selectively stimulate targeted cells without causing off-target effects. Several studies have reported that the overactivity of the amygdala area may play an important role in epilepsy. Minami et al. showed that the surgery to remove the amygdala area alone can be sufficient to eliminate epilepsy [47,48]. Additionally, the amygdala area attends the earliest stages in the epilepsy-induced process, with the most extensive damage after nerve agent exposure [49], which indicates that the amygdala area has an exceptionally high susceptibility to seizure-induced insults. Especially the basolateral nucleus of the amygdala has been demonstrated to play a primary role in generating widespread seizure epilepsy [50,51]. Therefore, modulating the activity of the amygdala area is important in epilepsy treatment. Besides, GABA could reduce neuron activities, and the proportion of GABAergic neurons is around 22 % in the amygdala area [52]. As a result, activating GABAergic neurons in a targeted manner without needing large amounts of energy or long stimulation durations could avoid the hyperexcitation and hypersynchronization of neurons and thereby also epileptic spikes. In our study, the high expression of Venus-mPrestin in GABAergic neurons was found after AAV-Venus-mPrestin injection, similar to a previous work by Aschauer et al. (2013) [53]. They transfected different subtypes of rAAV-GFP (AAV1, AAV2, AAV5, AAV6, AAV8, AAV9) into the mouse brain and found that in all transfected brain areas (striatum, hippocampus, and cortex), the AAV9-GFP signal in inhibitory neurons (GABA neurons) expressed with high intensity compared to other cell types. Although the exact mechanism is still unclear, one of the potential reasons is that the injection site of AAV-Venus-mPrestin was the amygdala area, which has a high portion of GABAergic neurons (~22 %) [52]. It might improve the probability that the GABAergic neurons were transfected by AAV-Venus-mPrestin.

While AAV vectors are not very immunogenic in different animals [54–56], injecting AAV at a high titer/dose still induces immune responses in local tissues and even whole bodies [57,58]. Our IHC evaluations revealed the presence of microglia in the area injected with AAV-Venus-mPrestin at 5 μl/rat. This result was similar to Gou et al.'s finding that administering high-titer AAV could disrupt the blood-brain barrier (BBB) and induce the infiltration of immune cells [57]. There are no significant differences between the healthy group and the groups injected with 1 or 3 μl of AAV-Venus-mPrestin, which implies that administering 3 μl of AAV-Venus-mPrestin is safe. Furthermore, US stimulation's cavitation, mechanical, and thermal effects can induce inflammation responses, cellular apoptosis, and microhemorrhages [59,60]. The acoustic parameters used in this study (acoustic pressure = 0.5 MPa, MI = 0.71, I_{SPTA} = 324.7 mW/cm^2, and I_{SPPA} = 8.1 W/cm^2) were below the FDA upper limits for a clinical trial (MI = 1.9, I_{SPTA} = 720 mW/cm^2) [61,62] and too low to induce potential tissue biohazards such as thermal or cavitation effects, for which the threshold is 40 MPa when microbubbles are not used [63]. In addition, no DNA damage or histological damage in the targeted amygdala area was observed in the histological sections with H&E or TUNEL staining. Together these findings indicate that our proposed sonogenetic tool is a safe strategy for stimulating brain neurons.

We found significant reductions in the epileptic spike counts in the delta, theta, and alpha bands following US stimulation of Venus-

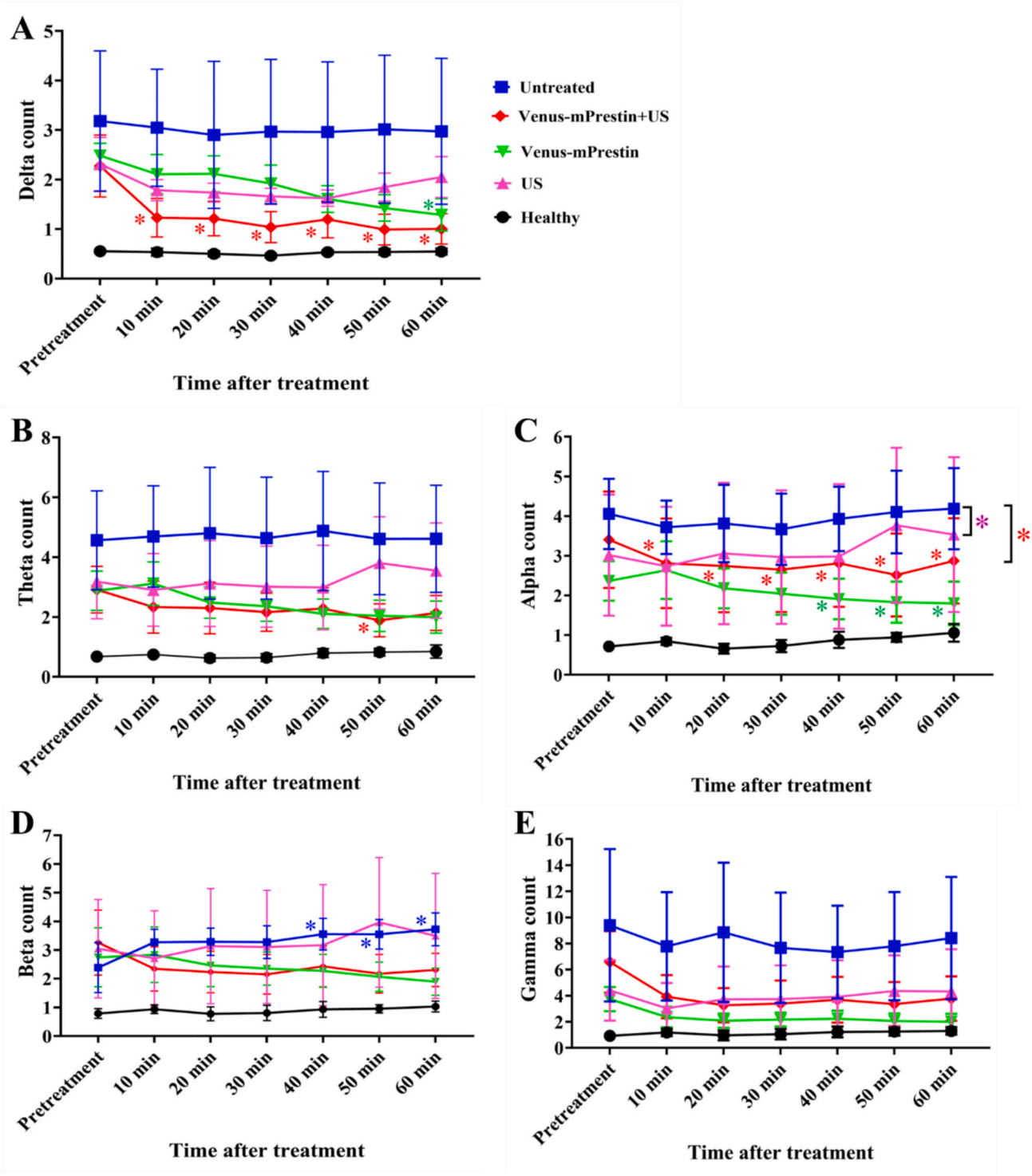

Fig. 6. Spike counts in different bands under different treatment conditions: (A) delta band, (B) theta band, (C) alpha band, (D) beta band, and (E) gamma band. Data are mean ± SEM values of five animal groups. Statistics: Two-way ANOVA, Tukey correction. *, $p < 0.05$. The asterisk color indicated the group marked with the corresponding color.

mPrestin-expressing GABAergic neurons. In contrast, the peak values in these bands increased significantly in untreated epileptic rats. Previous studies have found that epilepsy-induced changes in the delta, theta, and alpha bands result from the high synchronization of brain networks in different brain regions [36,37,64]. This suggests that the transmission of epileptic signals is suppressed by adjusting circuit connections or the characteristic path lengths of signal transduction, thereby mitigating epileptic seizures. Further research is required to confirm the correlation between the power of high-frequency bands in epilepsy brainwaves and Venus-mPrestin+US treatment. The relationship between neuronal connections and the role of Venus-mPrestin+US neuromodulation also needs to be further investigated. It is well known that GABA is an important neurotransmitter that can widely and synchronously modulate the activity of neurons in the brain, resulting in transient strong neuronal connections. Previous articles showed that powerful inhibitory circuits control the expression of conditioned responses in the amygdala,

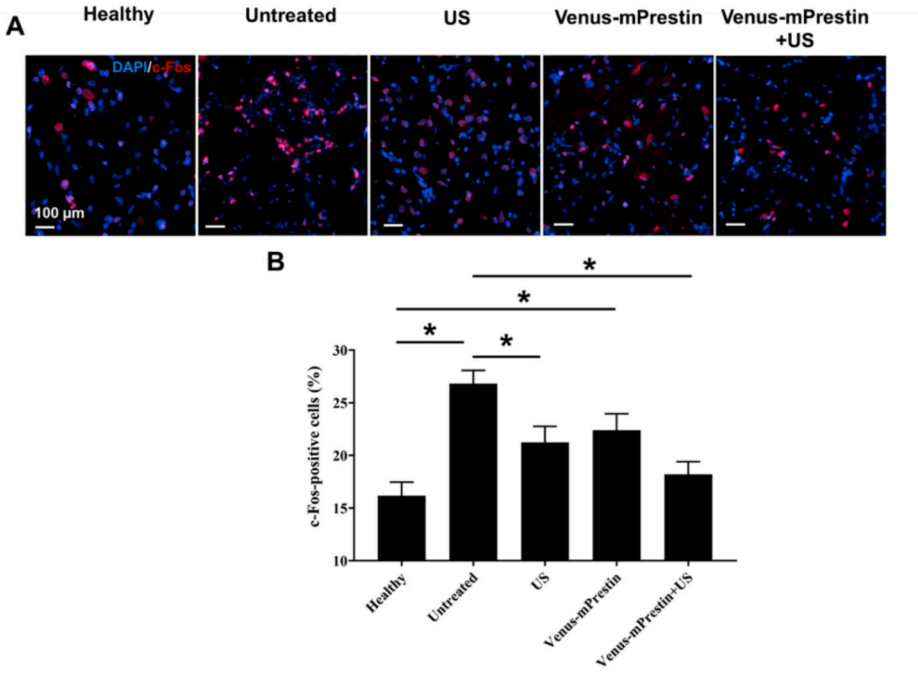

Fig. 7. (A) c-Fos IHC of rat brain sections from the healthy, untreated, US-only, Venus-mPrestin-only, and Venus-mPrestin+US groups are shown. (B) The percentages of c-Fos positive cells in the indicated conditions are shown as mean ± SEM. $n = 4$ rats per group. One-way ANOVA, Tukey correction: *, $p < 0.05$.

including inhibition from the prefrontal cortex and thalamus [65,66]. Our rs-fMRI data might support our hypothesis that only regions expressing the Venus-mPrestin are enhanced sensitive to US. However, this is the preliminary rs-fMRI readout on the Venus-mPrestin+US rat, more experiments need to be repeated to draw definitive conclusions.

This study has provided an innovative framework for inhibiting epileptic brainwaves. However, the proposed method still has several limitations, so further modifications may improve its efficacy. First, the observation time for the effects of epilepsy treatment should be increased so that the efficacy duration of the sonogenetic tool can be estimated. Second, we only applied the sonogenetic tool in an acute epilepsy animal model. Since chronic temporal epilepsy also often appears in humans, future studies should apply Venus-mPrestin+US in a chronic epilepsy animal model. Third, the amounts of GABA neurotransmitters present before, during, and after Venus-mPrestin+US should be monitored. Fourth, the mechanism underlying the role of Venus-mPrestin in epilepsy treatment should be investigated. Although the noninvasiveness of this technique represents a significant advantage, the reliance on viral delivery systems introduces several challenges that must be carefully considered. These challenges include (1) immunogenicity, strategies such as using less immunogenic viral serotypes, engineering viral vectors to evade immune detection, or implementing transient immunosuppression during delivery could be employed [67]; (2) Viral delivery route, combining microbubbles and US-induced BBB opening techniques, or US-responsive nanoparticles, may facilitate the noninvasive delivery of viruses into the targeted brain area without the obstacle of the BBB [3]; (3) Off-target effects, to minimize the potential for off-target effects and strategies such as using tissue-specific promoters or guided RNA technologies (*e.g.*, CRISPR-Cas systems) may improve the specificity of viral payload delivery to the intended cells [68].

5. Conclusions

This study has demonstrated a potential strategy for utilizing sonogenetics to modulate neuronal hyperexcitation in epileptic animals by targeting GABAergic neurons. Further investigations are required to elucidate the mechanisms underlying the effects of Venus-mPrestin in neuromodulation. Research aimed at improving gene delivery methods is also necessary. Further experiments to optimize US parameters for achieving long-term effects and enhancing the suppressive capabilities of Venus-mPrestin in epilepsy will be pursued.

Author contributions

All authors contributed extensively to this work. Conceived and designed the experiments: T.N·P., C.H.F., and C.K.Y. Performed the experiments: T.N.P., H.C.W., and Y.C.L.. Generated the DNA constructs: H. C.W.. and Y.C.L. T.N.P. performed the animal experiments under the supervisor of C.H.F. and C.K.Y. T.N.P. performed the fMRI experiments under the supervisor of H.L.L., C.H.F., and C.K.Y. T.N.P. and H.C.W. quantified the imaging results. Analyzed the data: T.N.P and C.H.F. Contributed reagents/materials/analysis tools: H.L.L, Y.C.L., and C.K.Y. Wrote the paper: T.N.P., C.H.F., and C.K.Y. The manuscript was written through the contributions of all authors. All authors have approved the final version of the manuscript.

Funding sources

This work was supported by the National Science and Technology Council, Taiwan (grant number NSTC 110-2221-E-007-019-MY3, NSTC 111-2221-E-007-019-MY3, and NSTC 112-2321-B-002-021 to C.K.Y.; NSTC 113-2628-B-007-003, NSTC 113-2740-B-007-001 to Y.C.L. and NSTC 113-2636-E-006-002 to C.H.F.).

CRediT authorship contribution statement

Thi-Nhan Phan: Writing – review & editing, Writing – original draft, Project administration, Methodology, Formal analysis, Data curation, Conceptualization. **Ching-Hsiang Fan:** Writing – review & editing, Writing – original draft, Validation, Resources, Project administration, Methodology, Formal analysis, Data curation, Conceptualization. **Hsien-Chu Wang:** Methodology, Formal analysis, Data curation. **Hao-Li Liu:** Resources, Methodology, Data curation. **Yu-Chun Lin:** Writing –

review & editing, Supervision, Resources, Methodology, Data curation, Conceptualization. **Chih-Kuang Yeh:** Writing – review & editing, Writing – original draft, Validation, Supervision, Resources, Project administration, Methodology, Data curation, Conceptualization.

Declaration of competing interest

The authors declare no competing financial interest.

Data availability

Data will be made available on request.

Acknowledgements

The authors gratefully acknowledge the support of Y.-J. Juan for his help with the rs-fMRI experiments and L.-D. Liao for his help with experiments.

Appendix A. Supplementary data

Supplementary data to this article can be found online at https://doi.org/10.1016/j.jconrel.2024.11.029.

References

[1] A.A. Asadi-Pooya, F. Brigo, S. Lattanzi, I. Blumcke, Adult epilepsy, Lancet 402 (2023) 412–424, https://doi.org/10.1016/S0140-6736(23)01048-6.
[2] D.M. Treiman, GABAergic mechanisms in epilepsy, Epilepsia 42 (2001) 8–12, https://doi.org/10.1046/j.1528-1157.2001.042Suppl.3008.x.
[3] C.-Y. Wu, C.-H. Fan, N.-H. Chiu, Y.-J. Ho, Y.-C. Lin, C.-K. Yeh, Targeted delivery of engineered auditory sensing protein for ultrasound neuromodulation in the brain, Theranostics 10 (2020) 3546–3561, https://doi.org/10.7150/thno.39786.
[4] Y.-S. Huang, C.-H. Fan, N. Hsu, N.-H. Chiu, C.-Y. Wu, C.-Y. Chang, B.-H. Wu, S.-R. Hong, Y.-C. Chang, A. Yan-Tang Wu, V. Guo, Y.-C. Chiang, W.-C. Hsu, L. Chen, C. Pin-Kuang Lai, C.-K. Yeh, Y.-C. Lin, Sonogenetic modulation of cellular activities using an engineered auditory-sensing protein, Nano Lett. 20 (2020) 1089–1100, https://doi.org/10.1021/acs.nanolett.9b04373.
[5] C.-H. Fan, K.-C. Wei, N.-H. Chiu, E.-C. Liao, H.-C. Wang, R.-Y. Wu, Y.-J. Ho, H.-L. Chan, T.-S.A. Wang, Y.-Z. Huang, T.-H. Hsieh, C.-H. Lin, Y.-C. Lin, C.-K. Yeh, Sonogenetic-based neuromodulation for the amelioration of Parkinson's disease, Nano Lett. 21 (2021) 5967–5976, https://doi.org/10.1021/acs.nanolett.1c00886.
[6] H.-C. Wang, T.-N. Phan, C.-L. Kao, C.-K. Yeh, Y.-C. Lin, Genetically encoded mediators for sonogenetics and their applications in neuromodulation, Front. Cell. Neurosci. 17 (2023), https://doi.org/10.3389/fncel.2023.1326279.
[7] N. Miyakawa, Y. Nagai, Y. Hori, K. Mimura, A. Orihara, K. Oyama, T. Matsuo, K. Inoue, T. Suzuki, T. Hirabayashi, T. Suhara, M. Takada, M. Higuchi, K. Kawasaki, T. Minamimoto, Chemogenetic attenuation of cortical seizures in nonhuman primates, Nat. Commun. 14 (2023) 1–11, https://doi.org/10.1038/s41467-023-36642-6.
[8] R.A. Poldrack, M.J. Farah, Progress and challenges in probing the human brain, Nature 526 (2015) 371–379, https://doi.org/10.1038/nature15692.
[9] K. Deisseroth, Optogenetics, Nat. Methods 8 (2011) 26–29, https://doi.org/10.1038/nmeth.f.324.
[10] X. Long, J. Ye, D. Zhao, S.J. Zhang, Magnetogenetics: remote non-invasive magnetic activation of neuronal activity with a magnetoreceptor, Sci. Bull. 60 (2015) 2107–2119, https://doi.org/10.1007/s11434-015-0902-0.
[11] S. Del Sol-Fernández, P. Martínez-Vicente, P. Gomollón-Zueco, C. Castro-Hinojosa, L. Gutiérrez, R.M. Fratila, M. Moros, Magnetogenetics: remote activation of cellular functions triggered by magnetic switches, Nanoscale 14 (2022) 2091–2118, https://doi.org/10.1039/d1nr06303k.
[12] J. French, V. Biton, H. Dave, K. Detyniecki, M.A. Gelfand, H. Gong, K. Liow, T. J. O'Brien, A. Sadek, B. DiVentura, B. Reich, J. Isojarvi, A eandomized phase 2b efficacy study in patients with seizure episodes with a predictable pattern using staccato® alprazolam for rapid seizure termination, Epilepsia 64 (2023) 374–385, https://doi.org/10.1111/epi.17441.
[13] W. Löscher, Is the Antiparasitic drug Ivermectin a suitable candidate for the treatment of epilepsy? Epilepsia 64 (2023) 553–566, https://doi.org/10.1111/epi.17511.
[14] Z. Han, C. Chen, A. Christiansen, S. Ji, Q. Lin, C. Anumonwo, C. Liu, S.C. Leiser, I. Meena, G. Aznarez, L.L. Isom Liau, Antisense oligonucleotides increase Scn1a expression and reduce seizures and SUDEP incidence in a mouse model of Dravet syndrome, Sci. Transl. Med. 12 (2020), https://doi.org/10.1126/SCITRANSLMED.AAZ6100.
[15] M.A. Nitsche, W. Paulus, Noninvasive brain stimulation protocols in the treatment of epilepsy: current state and perspectives, Neurotherapeutics 6 (2009) 244–250, https://doi.org/10.1016/j.nurt.2009.01.003.
[16] S. Ibsen, A. Tong, C. Schutt, S. Esener, S.H. Chalasani, Sonogenetics is a non-invasive approach to activating neurons in caenorhabditis elegans, Nat. Commun. 6 (2015) 1–12, https://doi.org/10.1038/ncomms9264.
[17] Z. Qiu, S. Kala, J. Guo, Q. Xian, J. Zhu, T. Zhu, X. Hou, K.F. Wong, M. Yang, H. Wang, L. Sun, Targeted neurostimulation in mouse brains with non-invasive ultrasound, Cell Rep. 32 (2020) 108033, https://doi.org/10.1016/j.celrep.2020.108033.
[18] J. Kubanek, P. Shukla, A. Das, S.A. Baccus, M.B. Goodman, Ultrasound elicits behavioral responses through mechanical effects on neurons and ion channels in a simple nervous system, J. Neurosci. 38 (2018) 3081–3091, https://doi.org/10.1523/JNEUROSCI.1458-17.2018.
[19] Y. Yang, C.P. Pacia, D. Ye, L. Zhu, H. Baek, Y. Yue, J. Yuan, M.J. Miller, J. Cui, J. P. Culver, M.R. Bruchas, H. Chen, Sonothermogenetics for noninvasive and cell-type specific deep brain neuromodulation, Brain Stimul. 14 (2021) 790–800, https://doi.org/10.1016/j.brs.2021.04.021.
[20] J. Zhu, Q. Xian, X. Hou, K.F. Wong, T. Zhu, Z. Chen, D. He, S. Kala, S. Murugappan, J. Jing, Y. Wu, X. Zhao, D. Li, J. Guo, Z. Qiu, L. Sun, The mechanosensitive ion channel Piezo1 contributes to ultrasound neuromodulation, Proc. Natl. Acad. Sci. 120 (2023) 2017, https://doi.org/10.1073/pnas.2300291120.
[21] Q. Xian, Z. Qiu, S. Murugappan, S. Kala, K.F. Wong, D. Li, G. Li, Y. Jiang, Y. Wu, M. Su, X. Hou, J. Zhu, J. Guo, W. Qiu, L. Sun, Modulation of deep neural circuits with sonogenetics, Proc. Natl. Acad. Sci. 120 (2023) 2017, https://doi.org/10.1073/pnas.2220575120.
[22] X. Shen, Z. Song, E. Xu, J. Zhou, F. Yan, Sensitization of nerve cells to ultrasound stimulation through piezo1-targeted microbubbles, Ultrason. Sonochem. 73 (2021) 105494, https://doi.org/10.1016/j.ultsonch.2021.105494.
[23] J. Heureaux, D. Chen, V.L. Murray, C.X. Deng, A.P. Liu, Activation of a bacterial mechanosensitive channel in mammalian cells, Cell. Mol. Bioeng. 7 (2014) 307–319, https://doi.org/10.1007/s12195-014-0337-8.Activation.
[24] M.L. Prieto, K. Firouzi, B.T. Khuri-Yakub, M. Maduke, Activation of Piezo1 but not NaV1.2 channels by ultrasound at 43 MHz, Ultrasound Med. Biol. 44 (2018) 1217–1232, https://doi.org/10.1016/j.ultrasmedbio.2017.12.020.
[25] J. Ye, S. Tang, L. Meng, X. Li, X. Wen, S. Chen, L. Niu, X. Li, W. Qiu, H. Hu, M. Jiang, S. Shang, Q. Shu, H. Zheng, S. Duan, Y. Li, Ultrasonic control of neural activity through activation of the mechanosensitive channel MscL, Nano Lett. 18 (2018) 4148–4155, https://doi.org/10.1021/acs.nanolett.8b00935.
[26] T. Yamaguchi, T. Hori, H. Hori, M. Takasaki, K. Abe, T. Taira, K. Ishii, K. Watanabe, Magnetic resonance–guided focused ultrasound ablation of hypothalamic hamartoma as a disconnection surgery: a case report, Acta Neurochir. 162 (2020) 2513–2517, https://doi.org/10.1007/s00701-020-04468-6.
[27] C.-Y. Wu, C.-H. Fan, N.-H. Chiu, Y.-J. Ho, Y.-C. Lin, C.-K. Yeh, Targeted delivery of engineered auditory sensing protein for ultrasound neuromodulation in the brain, Theranostics 10 (2020) 3546–3561, https://doi.org/10.7150/thno.39786.
[28] M. Kinoshita, N. McDannold, F.A. Jolesz, K. Hynynen, Noninvasive localized delivery of herceptin to the mouse brain by MRI-guided focused ultrasound-induced blood-brain barrier disruption, Proc. Natl. Acad. Sci. USA 103 (2006) 11719–11723, https://doi.org/10.1073/pnas.0604318103.
[29] J. Zou, L. Meng, Z. Lin, Y. Qiao, C. Tie, Y. Wang, X. Huang, T. Yuan, Y. Chi, W. Meng, L. Niu, Y. Guo, H. Zheng, Ultrasound neuromodulation inhibits seizures in acute epileptic monkeys, IScience 23 (2020) 101066, https://doi.org/10.1016/j.isci.2020.101066.
[30] P.-C. Chu, H.-Y. Yu, C.-C. Lee, R. Fisher, H.-L. Liu, Pulsed-focused ultrasound provides long-term suppression of epileptiform bursts in the Kainic acid-induced epilepsy rat model, Neurotherapeutics 19 (2022) 1368–1380, https://doi.org/10.1007/s13311-022-01250-7.
[31] X. Jiang, O. Savchenko, Y. Li, S. Qi, T. Yang, W. Zhang, J. Chen, A review of low-intensity pulsed ultrasound for therapeutic applications, IEEE Trans. Biomed. Eng. 66 (2019) 2704–2718, https://doi.org/10.1109/TBME.2018.2889669.
[32] H.I. Elsner, E.B. Lindblad, Ultrasonic degradation of DNA, Dna 8 (1989) 697–701, https://doi.org/10.1089/dna.1989.8.697.
[33] R.Q. Huang, C.L. Bell-Horner, M.I. Dibas, D.F. Covey, J.A. Drewe, G.H. Dillon, Pentylenetetrazole-induced inhibition of recombinant gamma-aminobutyric acid type A (GABA(A)) receptors: mechanism and site of action, J. Pharmacol. Exp. Ther. 298 (2001) 986–995. http://www.ncbi.nlm.nih.gov/pubmed/11504794.
[34] J. Glykys, V. Dzhala, K. Egawa, T. Balena, Y. Saponjian, K.V. Kuchibhotla, B. J. Bacskai, K.T. Kahle, T. Zeuthen, K.J. Staley, Local impermeant anions establish the neuronal chloride concentration, Science (80-.) 343 (2014) 670–675, https://doi.org/10.1126/science.1245423.
[35] E.Y. Proskurina, A.V. Zaitsev, Regulation of potassium and chloride concentrations in nervous tissue as a method of anticonvulsant therapy, J. Evol. Biochem. Physiol. 58 (2022) 1275–1292, https://doi.org/10.1134/S0022093022050015.
[36] W.E. Haley, Freeman, shift in interictal relative gamma power as a novel biomarker for drug response in two mouse models of absence epilepsy, Physiol. Behav. 176 (2018) 139–148, https://doi.org/10.1111/epi.13265.Shift.
[37] A. Maheshwari, A. Akbar, M. Wang, R.L. Marks, K. Yu, S. Park, B.L. Foster, J. L. Noebels, Persistent aberrant cortical phase–amplitude coupling following seizure treatment in absence epilepsy models, J. Physiol. 595 (2017) 7249–7260, https://doi.org/10.1113/JP274696.
[38] P.C. Chu, H.Y. Yu, C.C. Lee, R. Fisher, H.L. Liu, Pulsed-focused ultrasound provides long-term suppression of epileptiform bursts in the Kainic acid-induced epilepsy rat model, Neurotherapeutics 19 (2022) 1368–1380, https://doi.org/10.1007/s13311-022-01250-7.
[39] E. Kim, H.C. Kim, J. Van Reet, M. Böhlke, S.S. Yoo, W. Lee, Transcranial focused ultrasound-mediated unbinding of phenytoin from plasma proteins for suppression of chronic temporal lobe epilepsy in a rodent model, Sci. Rep. 13 (2023) 1–15, https://doi.org/10.1038/s41598-023-31383-4.

[40] M. Zhang, B. Li, Y. Liu, R. Tang, Y. Lang, Q. Huang, J. He, Different modes of low-frequency focused ultrasound-mediated attenuation of epilepsy based on the topological theory, Micromachines 12 (2021) 1–19, https://doi.org/10.3390/mi12081001.
[41] H. Hakimova, S. Kim, K. Chu, S.K. Lee, B. Jeong, D. Jeon, Ultrasound stimulation inhibits recurrent seizures and improves behavioral outcome in an experimental model of mesial temporal lobe epilepsy, Epilepsy Behav. 49 (2015) 26–32, https://doi.org/10.1016/j.yebeh.2015.04.008.
[42] S.-G. Chen, C.-H. Tsai, C.-J. Lin, C.-C. Lee, H.-Y. Yu, T.-H. Hsieh, H.-L. Liu, Transcranial focused ultrasound pulsation suppresses pentylenetetrazol induced epilepsy in vivo, Brain Stimul. 13 (2020) 35–46, https://doi.org/10.1016/j.brs.2019.09.011.
[43] C. Lee, C. Chou, F. Hsiao, Y. Chen, C. Lin, C. Chen, S. Peng, H. Liu, H. Yu, Pilot study of focused ultrasound for drug-resistant epilepsy, Epilepsia 63 (2022) 162–175, https://doi.org/10.1111/epi.17105.
[44] Z. Lin, L. Meng, J. Zou, W. Zhou, X. Huang, S. Xue, T. Bian, T. Yuan, L. Niu, Y. Guo, H. Zheng, Non-invasive ultrasonic neuromodulation of neuronal excitability for treatment of epilepsy, Theranostics 10 (2020) 5514–5526, https://doi.org/10.7150/thno.40520.
[45] B.K. Min, A. Bystritsky, K.I. Jung, K. Fischer, Y. Zhang, L.S. Maeng, S. In Park, Y. A. Chung, F.A. Jolesz, S.S. Yoo, Focused ultrasound-mediated suppression of chemically-induced acute epileptic EEG activity, BMC Neurosci. 12 (2011) 23, https://doi.org/10.1186/1471-2202-12-23.
[46] T. Kim, T. Kim, J. Joo, I. Ryu, S. Lee, E. Park, Y.-M. Shon, Modulation of EEG frequency characteristics by low-intensity focused ultrasound stimulation in a pentylenetetrazol-induced epilepsy model, IEEE Access 9 (2021) 59900–59909, https://doi.org/10.1109/ACCESS.2021.3073506.
[47] R. Jooma, H.S. Yeh, M.D. Privitera, D. Rigrish, M. Gartner, Seizure control and extent of mesial temporal resection, Acta Neurochir. 133 (1995) 44–49, https://doi.org/10.1007/BF01404946.
[48] N. Minami, M. Morino, T. Uda, T. Komori, Y. Nakata, N. Arai, E. Kohmura, I. Nakano, Surgery for amygdala enlargement with mesial temporal lobe epilepsy: pathological findings and seizure outcome, J. Neurol. Neurosurg. Psychiatry 86 (2015) 887–894, https://doi.org/10.1136/jnnp-2014-308383.
[49] T.M. Shih, S.M. Duniho, J.H. McDonough, Control of nerve agent-induced seizures is critical for neuroprotection and survival, Toxicol. Appl. Pharmacol. 188 (2003) 69–80, https://doi.org/10.1016/S0041-008X(03)00019-X.
[50] Kinam Park, Pathology and pathophysiology of the amygdala in Epileptogenesis and epilepsy, Bone 23 (2014) 1–7, https://doi.org/10.1016/j.eplepsyres.2007.11.011.Pathology.
[51] L. White, J. Price, The functional anatomy of limbic status epilepticus in the rat. II. The effects of focal deactivation, J. Neurosci. 13 (1993) 4810–4830, https://doi.org/10.1523/JNEUROSCI.13-11-04810.1993.
[52] V.K. Vereczki, K. Müller, É. Krizsán, Z. Máté, Z. Fekete, L. Rovira-Esteban, J. M. Veres, F. Erdélyi, N. Hájos, Total number and ratio of GABAergic neuron types in the mouse lateral and basal amygdala, J. Neurosci. 41 (2021) 4575–4595, https://doi.org/10.1523/JNEUROSCI.2700-20.2021.
[53] D.F. Aschauer, S. Kreuz, S. Rumpel, Analysis of transduction efficiency, tropism and axonal transport of AAV serotypes 1, 2, 5, 6, 8 and 9 in the mouse brain, PLoS One 8 (2013) e76310, https://doi.org/10.1371/journal.pone.0076310.
[54] R.W. Herzog, J.N. Hagstrom, S.-H. Kung, S.J. Tai, J.M. Wilson, K.J. Fisher, K. A. High, Stable gene transfer and expression of human blood coagulation factor IX after intramuscular injection of recombinant adeno-associated virus, Proc. Natl. Acad. Sci. 94 (1997) 5804–5809, https://doi.org/10.1073/pnas.94.11.5804.
[55] G.P. Niemeyer, R.W. Herzog, J. Mount, V.R. Arruda, D.M. Tillson, J. Hathcock, F. W. van Ginkel, K.A. High, C.D. Lothrop, Long-term correction of inhibitor-prone hemophilia B dogs treated with liver-directed AAV2-mediated factor IX gene therapy, Blood 113 (2009) 797–806, https://doi.org/10.1182/blood-2008-10-181479.
[56] S.R.P. Kumar, J. Xie, S. Hu, J. Ko, Q. Huang, H.C. Brown, A. Srivastava, D. M. Markusic, C.B. Doering, H.T. Spencer, A. Srivastava, G. Gao, R.W. Herzog, Coagulation factor IX gene transfer to non-human Primates using engineered AAV3 capsid and hepatic optimized expression cassette, Mol. Ther. Methods Clin. Dev. 23 (2021) 98–107, https://doi.org/10.1016/j.omtm.2021.08.001.
[57] Y. Guo, J. Chen, W. Ji, L. Xu, Y. Xie, S. He, C. Lai, K. Hou, Z. Li, G. Chen, Z. Wu, High-titer AAV disrupts cerebrovascular integrity and induces lymphocyte infiltration in adult mouse brain, Mol. Ther. Methods Clin. Dev. 31 (2023) 101102, https://doi.org/10.1016/j.omtm.2023.08.021.
[58] L. Huang, J. Wan, Y. Wu, Y. Tian, Y. Yao, S. Yao, X. Ji, S. Wang, Z. Su, H. Xu, Challenges in adeno-associated virus-based treatment of central nervous system diseases through systemic injection, Life Sci. 270 (2021) 119142, https://doi.org/10.1016/j.lfs.2021.119142.
[59] D. Janssen, J. Stolk, N. Verdonschot, Finite element analysis of the Long-term fixation strength of cemented ceramic cups, Proc. Inst. Mech. Eng. Part H J. Eng. Med. 220 (2006) 533–539, https://doi.org/10.1243/09544119JEIM61.
[60] W.J. Elias, D. Huss, T. Voss, J. Loomba, M. Khaled, E. Zadicario, R.C. Frysinger, S. A. Sperling, S. Wylie, S.J. Monteith, J. Druzgal, B.B. Shah, M. Harrison, M. Wintermark, A pilot study of focused ultrasound Thalamotomy for essential tremor, N. Engl. J. Med. 369 (2013) 640–648, https://doi.org/10.1056/nejmoa1300962.
[61] F.A. Duck, Acoustic saturation and output regulation, Ultrasound Med. Biol. 25 (1999) 1009–1018, https://doi.org/10.1016/S0301-5629(99)00038-1.
[62] T. Deffieux, Y. Younan, N. Wattiez, M. Tanter, P. Pouget, J.F. Aubry, Low-intensity focused ultrasound modulates monkey Visuomotor behavior, Curr. Biol. 23 (2013) 2430–2433, https://doi.org/10.1016/j.cub.2013.10.029.
[63] D. Dalecki, Mechanical bioeffects of ultrasound, Annu. Rev. Biomed. Eng. 6 (2004) 229–248, https://doi.org/10.1146/annurev.bioeng.6.040803.140126.
[64] M. Zhang, B. Li, X. Lv, S. Liu, Y. Liu, R. Tang, Y. Lang, Q. Huang, J. He, Low-intensity focused ultrasound-mediated attenuation of acute seizure activity based on EEG brain functional connectivity, Brain Sci. 11 (2021), https://doi.org/10.3390/brainsci11060711.
[65] G.J. Quirk, D.R. Gehlert, Inhibition of the amygdala: key to pathological states? Ann. N. Y. Acad. Sci. 985 (2003) 263–272, https://doi.org/10.1111/j.1749-6632.2003.tb07087.x.
[66] P. Das, A.H. Kemp, B.J. Liddell, K.J. Brown, G. Olivieri, A. Peduto, E. Gordon, L. M. Williams, Pathways for fear perception: modulation of amygdala activity by thalamo-cortical systems, Neuroimage 26 (2005) 141–148, https://doi.org/10.1016/j.neuroimage.2005.01.049.
[67] Y.K. Chan, S.K. Wang, C.J. Chu, A. Copland, J. Alexander, H.C. Verdera, J. J. Chiang, M. Sethi, M.K. Wang, W.J.N. Jr, Y. Chan, E.T. Lim, A.R. Graveline, M. Sanchez, R.F. Boyd, T.S. Vihtelic, R. Gian, C.O. Inciong, J.M. Slain, P. J. Alphonse, Y. Xue, L.R. Robinson-mccarthy, J.M. Tam, M.H. Jabbar, B. Sahu, J. F. Adeniran, P.W.L. Tai, J. Xie, T.B. Krause, A. Vernet, A.D. Dick, F. Mingozzi, M. A. Mccall, L. Constance, Engineering Adeno-Associated Viral Vectors to evade innate immune and inflammatory responses 13, 2021, pp. 1–34, https://doi.org/10.1126/scitranslmed.abd3438.Engineering.
[68] A. Sandoval, H. Elahi, J.E. Ploski, Genetically engineering the nervous system with CRISPR-Cas, Eneuro 7 (2020), https://doi.org/10.1523/ENEURO.0419-19.2020.ENEURO.0419-19.2020.